# Enasidenib Induces Acute Myeloid Leukemia Cell Differentiation to Promote Clinical Response

**One Sentence Summary:** Enasidenib promotes hematopoietic differentiation to induce clinical responses in *IDH2*-mutant Acute Myeloid Leukemia that are modulated by co-occurring mutations.

**Authors:** Michael D. Amatangelo[1]†, Lynn Quek[2]†, Alan Shih[3]†, Eytan M. Stein[3], Mikhail Roshal[3], Stephane de Botton[4], Benoit Marteyn[5], Noushin Rahnamay Farnoud[6], Muriel David[7], Bin Wu[8], Katharine E. Yen[8], Martin S. Tallman[3], Elli Papaemmanuil[6,9], Virginie Lacronique-Penard[4], Anjan Thakurta[1]*, Paresh Vyas[2]*, Ross L. Levine[3,6,10]*

†These authors contributed equally to this work

*To whom correspondence should be addressed: Ross Levine (leviner@mskcc.org), Paresh Vyas (paresh.vyas@imm.ox.ac.uk) and Anjan Thakurta (athakurta@celgene.com)

**Affiliations:**

[1]Celgene Corporation, Summit, NJ, [2]Medical Research Council Molecular Hematology Unit, Oxford Comprehensive Biomedical Research Centre, Weatherall Institute of Molecular Medicine and Department of Hematology, Oxford University Hospital NHS Foundation Trust, Oxford, United Kingdom, University of Oxford, Oxford, United Kingdom, [3]Department of Medicine, Leukemia Service, Memorial Sloan Kettering Cancer Center, New York, NY, [4]Hématologie Clinique, Institut Gustave Roussy, Université Paris-Saclay, Villejuif, France, [5]Unité de Pathogénie Microbienne Moléculaire, Institut Pasteur, Paris, France, [6]Center for Hematologic

Malignancies, Memorial Sloan Kettering Cancer Center, New York, NY, [7]Institut Gustave Roussy, Université Paris-Saclay, 94805 Villejuif, France, [8]Agios Pharmaceuticals, Cambridge, MA, [9]Center for Molecular Oncology and Department of Epidemiology and Biostatistics, Memorial Sloan Kettering Cancer Center, New York, NY, [10]Human Oncology and Pathogenesis Program, Memorial Sloan Kettering Cancer Center, New York, NY

**Abstract:** Recurrent mutations at R140 and R172 in *isocitrate dehydrogenase 2* (*IDH2*) occur in many cancers, including ~12% of acute myeloid leukemia (AML). In preclinical models these mutations cause accumulation of the oncogenic metabolite R-2-hydroxyglutarate (2-HG) and induce hematopoietic differentiation block. Single-agent enasidenib (AG-221/CC-90007), a selective mutant IDH2 (mIDH2) inhibitor, produced an overall response rate of 40.3% in relapsed/refractory AML patients with *mIDH2* in a phase 1 trial. However, its mechanism of action and biomarkers associated with response remain unclear. Here, we measured 2-HG, *mIDH2* allele burden, and co-occurring somatic mutations in sequential patient samples from the clinical trial and correlated these with clinical response. Furthermore, we used flow cytometry to assess inhibition of mIDH2 on hematopoietic differentiation. We observed potent 2-HG suppression in both R140- and R172 AML subtypes, with different kinetics, which preceded clinical response. Suppression of 2-HG alone did not predict response, as most non-responding patients also exhibited 2-HG suppression. In a subset of patients, m*IDH2* allele burden decreased with response. Conversely, complete remission with persistence of *mIDH2* and normalization of hematopoietic stem and progenitor compartments with emergence of functional m*IDH2* neutrophils was more commonly observed. Co-occurring mutations in *NRAS* and other MAPK pathway effectors were enriched in non-responding patients, consistent with RAS signaling contributing to primary therapeutic resistance. Together, these data support differentiation as the main mechanism of enasidenib efficacy in relapse/refractory AML patients and provide insights into resistance mechanisms to inform future mechanism-based combination treatment studies.

**Key Points:**

- Enasidenib treatment potently inhibits mIDH2 and results in leukemic cell differentiation with emergence of functional mIDH2 neutrophils in rrAML patients.

- RAS pathway mutations, and increased mutational burden overall, are associated with a decreased response rate to mIDH2 inhibition.

**Introduction (206)**

Somatic mutations in the *isocitrate dehydrogenase 2 (IDH2)* gene occur at conserved arginine residues (R140 and R172). These mutant proteins possess neomorphic enzymatic activity resulting in R-2-hydroxyglutarate (2-HG) accumulation [1-4]. 2-HG competitively inhibits a set of alpha-ketoglutarate-dependent enzymes including the TET family of 5-methylcytosine (5mC) hydroxylases and the Jumonji-C domain histone demethylases [5,6]. This leads to DNA hypermethylation [7], increased repressive histone methylation [6], and impaired hematopoietic differentiation. Accordingly, inhibition of mutant IDH2 (mIDH2) reduces 2-HG levels and restores hematopoietic differentiation *in vitro* [6,8-10].

Although both mutations are characterized by neomorphic enzymatic activity, myeloid malignancies with R140 and R172 IDH2 mutations are distinct entities with respect to clinical outcome, co-mutational profile, and molecular classification [11-13]. In preclinical studies, enasidenib (AG-221/CC-90007), a small-molecule inhibitor of mIDH2, reduced serum 2-HG, DNA hypermethylation, and repressive histone marks, and promoted hematopoietic differentiation in R140 and R172 mIDH2 models [14-17]. In a phase 1/2 clinical trial, enasidenib demonstrated clinical activity in patients with both R140 and R172 mIDH2 relapsed/refractory AML (rrAML) with an overall response rate (ORR) of 40.3% [18]. Here, we analyzed patient samples from this study to elucidate the mechanisms of action of enasidenib in R140 and R172 mIDH2 rrAML and to identify response biomarkers to targeted mIDH2 therapy.

**Materials and Methods (1150)**

*Study Participants and Treatment*

Analyses were performed on rrAML patient samples collected from the AG-221-C-001 study with informed consent. Patients were enrolled with *IDH2* mutations detected by local testing. A retrospective central in vitro diagnostic test confirmed mutation status with a concordance rate above 95%. Enasidenib was administered to patients as described in the approved study protocol. Patient cohort characteristics are described elsewhere [18]. Patient sample disposition highlighting samples analyzed in each assay is supplied in **Figure S5.**

*Measurement and Analysis of 2-hydroxyglutarate (2-HG)*

Serum samples were collected from patients at screening within 28 days before the first dose of enasidenib and/or pre-dose on day 1 of each treatment cycle. 2-HG concentration was determined by liquid chromatography tandem mass spectrometry by Covance, Inc (formerly Tandem Labs) according to their validated method. Baseline 2-HG was determined to be either the average of the screening sample and the pre-dose cycle 1 sample, or either sample if both were not available. Maximum suppression of 2-HG levels was determined by comparing the lowest level of 2-HG observed on-treatment to baseline 2-HG level. Time to maximum suppression was the first time point where 2-HG level was within 5% of maximum suppression for that patient.

*Sysmex OncoBeam™ Digital Polymerase Chain Reaction*

Bone marrow and/or peripheral blood samples were collected at screening 28 days before the first dose of enasidenib or after treatment and processed to peripheral blood mononuclear cells (PBMC) and bone marrow mononuclear cells (BMMCs). Mutant *IDH2* variant allele frequency (VAF) in samples was determined using Sysmex BEAMing technology. Briefly, DNA was extracted from samples and multiple loci were pre-amplified in a multiplex PCR reaction. Pre-

amplified DNA fragments were then amplified with nested primers in an emulsion PCR reaction on the surface of magnetic beads in water–in-oil emulsions. Fluorescently labeled probes specific to the mutation and to the wild-type sequence of interest, respectively, were hybridized to the uncovered DNA fragments on the bead surface. Fluorescently labeled beads were quantified using flow cytometry. Mutant *IDH2* VAF was determined as the fraction of beads carrying mutant DNA fragments to those carrying wild-type DNA fragments per sample.

*Minimal Residual Disease (MRD) Blast Percentage Determination and mIDH2 Assessment*

Multi-parameter flow cytometry (MFC) was performed on marrow aspirates using three ten-"color" panels (**Table S4**) at diagnosis and at day 1 of each 28-day cycle. Abnormal populations were identified by visual assessment of antigen expression as described previously [19,20]. Briefly, up to 1.5 million cells from freshly drawn bone marrow aspirate were stained with the three panels, washed and acquired on a FACS-Canto-10 cytometer (BD Biosciences, San Jose CA). The results were analyzed using custom Woodlist software (generous gift of Wood BL, University of Washington). Following flow-MRD assessment samples were lysed and assessed for m*IDH2* as part a 28-gene amplicon capture-based NGS assay at Memorial Sloan Kettering Cancer Center.

*Hematopoietic Immunophenotyping and mIDH2 Assessment in Flow-Sorted Cells*

BMMC fractions from normal donors (N=12) or rrAML samples (N=9) stored as viably-frozen cells were thawed, washed and stained for FACS analysis on either a BD LSR Fortessa or BD FACSAria Fusion (Becton Dickinson, Oxford UK). Antibodies used in the immunophenotyping panel were: in the lineage (lin) depletion 'cocktail': anti-CD2, anti-CD3, anti-CD4, anti-CD8a, anti-CD10, anti-CD19, anti-CD20 and anti-CD235a; anti-CD34; CD117; and 7-aminoactinomycin D (7AAD, Becton Dickinson, UK) was used as a live/dead stain. Details of each antibody/ streptavidin analysis are listed in **Table S5.** FACS-sorted fractions (> 95% purity)

of lin-ve CD34-CD117- cells, which represent mature myelomonocytic cells, and unsorted mononuclear cells were processed for genomic DNA (gDNA). In samples with less than $10^4$ cells sorted, whole genome amplification (WGA, RepliG, Qiagen UK) was carried out on directly lysed sorted cells. WGA was also performed on gDNA from additional samples where extracted gDNA was inadequate. Analyses of m*IDH2* at R140 and R172 codons were carried out by PCR of exon 4 of the *IDH2* gene. Illumina MiSeq adapters were added by a second round of PCR, followed by NGS using a MiSeq (Illumina, UK). Sequencing reads with a Phred score of less than 30 were excluded from analysis. Mutant VAF was determined as the number of mutant reads divided by total number of reads.

*Phagocytosis Assay*

Neutrophils were collected from fresh citrated venous blood (45 mL) by centrifugation, red blood cell sedimentation and Percoll gradient cell separation. Purified neutrophils ($1 \times 10^6$) were incubated with 3 µL fluorescent green latex beads (Sigma, France) for 15 minutes at 37°C in 1 mL RPMI medium supplemented with 10% heat-inactivated fetal bovine serum (Sigma). After three washes with PBS, cells were fixed in 3.3 % paraformaldehyde and stained with DAPI. Fluorescent-labelled cells were observed using a laser-scanning TCS SP5 confocal microscope (Leica, France). The percentage of neutrophils containing latex beads was calculated by scoring 5 different fields of view for each sample.

*FoundationOne® Heme Panel*

Analysis of samples by the FoundationOne® Heme panel was conducted in a clinical laboratory improvement amendments (CLIA)-certified lab by Foundation Medicine, Inc. Briefly, fresh bone marrow and/or peripheral blood samples were collected from patients and DNA and RNA were extracted the day after by Foundation Medicine, Inc. Nucleic acid libraries were prepared and captured using custom bait-sets targeting 405 cancer-related genes by DNA-sequencing (DNA-

seq), and 265 frequently rearranged genes by RNA-sequencing (RNA-seq) and sequenced to high depth using Illumina HiSeq. Genes included in this analysis encode known or likely targets of therapies, either approved or in clinical trials, or are otherwise known drivers of oncogenesis published in the literature[21]. VAF was calculated as number of reads aligned over mutated nucleotide with mutation, over the number of reads aligned over mutated nucleotide with wild-type nucleotide. Mutational burden was calculated as noted by either: 1) the total sum of all known and likely somatic mutations identified by FoundationOne® Heme panel or 2) the sum of all genes that were identified with known and likely somatic mutations identified by FoundationOne® Heme panel.

*Statistical Analysis*

Where applicable, statistical analyses were performed using with GraphPad Prism software using statistical methods noted in figure and table legends.. Analysis of mutational associations with either overall response rate (ORR) or complete remission rate (CR) was assessed through a two-tailed Fisher's Exact test on a 2 x 2 contingency table analyzing the sum of patients achieving a response (For ORR responder defined as response ≥ PR versus non-responder defined as response < PR; for CR responder defined as response = CR versus non responder defined as response < CR) versus presence of mutation in a gene identified by FoundationOne® Heme versus absence of any alteration in same gene. Statistical associations between prognostic risk groups and response were assessed using a two-tailed Chi-square test for trend on a 3 x 2 contingency table analyzing the sum of patients achieving a response (response ≥ PR versus < PR for ORR or CR versus < CR for CR) versus classification as favorable, intermediate or adverse risk according to criteria as noted in text.

**Results (1856)**

*mIDH2 Inhibition Is Associated with Potent Reduction of 2-HG in mIDH2 AML*

We first assessed 2-HG levels in 125 rrAML patients with available data prior to enasidenib treatment and subsequently every 28 days during therapy. Median 2-HG suppression among patients, (defined as the maximum extent of suppression compared to pre-therapy in each patient), was 90.6% with a maximum of 100% (below detection limit), consistent with potent target inhibition. 2-HG suppression in patients with R172 mIDH2 was less than in patients with R140 mIDH2 rrAML (median suppression of 70.9% and 94.9%, respectively [$p < 0.001$]); consistent with preclinical data and an interim analysis of samples from patients with advanced hematological malignancies (**Fig. 1A**) [14-16,22-24].

We next assessed 2-HG suppression in patients dosed with <100mg, 100mg or >100mg enasidenib daily. Although we observed a trend towards greater 2-HG suppression at higher doses in R140 mIDH2 patients, there were no statistical differences in maximal 2-HG suppression among the three dosing groups ($p = 0.054$ for <100mg vs 100mg and $p = 0.094$ for 100mg vs >100mg) (**Fig. 1B**). In R172 mIDH2 patients, 2-HG suppression was more variable across dosing groups (95% CI: 43.9%-102.9%, 10.7%-61.0% and 62.5%- 82.7% in the <100mg, 100mg, and >100mg dosing groups, respectively). A statistical difference in 2-HG suppression was observed between 100mg and >100mg dosing cohorts. However, the 100mg group was confounded by 4 patients (2 responders and 2 non-responders) whose 2-HG levels increased and no statistical difference was found in 2-HG suppression between <100mg vs >100mg dosing groups ($p = 0.152$ for <100mg vs 100mg, $p = 0.022$ for 100mg vs >100mg and $p = 0.955$ for <100mg vs >100mg). Furthermore, response rates for R172 mIDH2 patients were not statistically different between the 100mg and >100mg dose groups analyzed (ORR 44.0% and 58.8%, respectively, $p = 0.530$, Fisher's exact test), suggesting no additional clinical benefit for R172 mIDH2 patients in dosing above 100mg. Together, 2-HG suppression and efficacy data

indicate that the 100mg enasidenib dose is biologically and therapeutically active in rrAML patients with m*IDH2*, regardless of the specific mutation.

We next assessed the relationship between pre-enasidenib therapy 2-HG levels and clinical response. We observed no significant difference in baseline 2-HG levels between patients achieving a complete remission (CR), patients obtaining any response (R = CR with incomplete hematologic recovery [CRi], CR with incomplete platelet count recovery [CRp], morphologic leukemia-free state or partial remission) and patients who did not respond (NR = stable disease or progressive disease) (**Fig. 1C**). We assessed whether timing of pharmacodynamic response, defined as maximal 2-HG suppression, correlated to best clinical response. Although the mean cycle number to maximal 2-HG suppression, best response (BR) and CR was ~1 treatment cycle later in R172 versus R140 patients (3 versus 2 cycles for maximal 2-HG suppression and BR, and 6 versus 5 cycles for CR) (**Fig. 1D**), the ORR and CR rates for patients with R172 and R140 mutations were not statistically different [18]. These data demonstrate the kinetics of target 2-HG inhibition parallel the kinetics of clinical response without effect on response attainment.

*Clinical Responses to mIDH2 Inhibition Do Not Correlate with mIDH2 Allele Burden*

We evaluated whether m*IDH2* allele burden at baseline or changes on-therapy correlated with response to enasidenib. Quantitation of m*IDH2* variant allele frequency (VAF) at screening and on-therapy was performed on unsorted samples using digital PCR and next generation sequencing (NGS). We observed a significant correlation between digital PCR and NGS for 45 matched patient samples run on both assays ($R^2 = 0.59$, $p < 0.0001$) (**Fig. S1**). m*IDH2* allele burden was highly heterogeneous among patients, ranging from low-level mutant positivity to fully clonal (~50%) (**Fig. 2A and Fig. S2A**). Notably, no association between *mIDH2* VAF at screening and clinical response was observed and patients achieving CR had both low and high m*IDH2* burden. When changes in absolute m*IDH2* VAF from screening to best response were analyzed, more responding patients had a decrease in m*IDH2* VAF than an increase, however,

only one-half of the patients showed a VAF change of more than 5% points (**Fig. 2B and Fig. S2B-C**). Similar to recent results reported for a subset of m*IDH1* AML patients treated with an mIDH1 inhibitor, longitudinal analysis by digital PCR in our cohort identified 9/29 CR patients where m*IDH2* became undetectable with enasidenib treatment [25]. Interestingly, all nine patients were R140 m*IDH2* rrAML subtype (50% of the 18 R140 CR patients). In eight of these patients, m*IDH2* remained undetectable with continued treatment, consistent with persistent molecular remission (**Fig. 2C**). In four of these patients, baseline m*IDH2* VAF was <5%, consistent with loss of a minor m*IDH2* subclone with therapy, and in the remaining patients we observed loss of a more substantive *mIDH2* clone in the setting of CR. No significant difference was observed in an initial analysis of event-free survival between patients achieving molecular remission versus patients achieving CR without molecular remission (295.9 versus 259.9 days, respectively, p = 0.784). Finally, we assessed the relationship between two measures of leukemic burden: bone marrow blast count (flow cytometry) and m*IDH2* VAF (genetic) in nine additional patients who responded to enasidenib (**Fig. 2D**). In six of these patients we observed marked blast count decreases to near 0% in aspirates with concomitant m*IDH2* VAF above 10%. This data demonstrates that m*IDH2* cells persist in most patients achieving CR and a reduction in m*IDH2* allele burden during treatment is neither necessary nor sufficient for clinical response to enasidenib.

*Clinical Response to mIDH2 Inhibition Is Associated with Induction of Myeloid Differentiation*

Given that a reduction in m*IDH2* VAF was not required for CR, we hypothesized that enasidenib might induce clinical response by promoting leukemic cell differentiation. We measured the magnitude of different immunophenotypic compartments in the hematopoietic hierarchy, before and during treatment, in five m*IDH2* AML patients who achieved CR or PR (**Fig. 3A-B**). Prior to treatment, all five patients had expanded myeloid leukemic progenitor or precursor populations. Enasidenib treatment resulted in near normalization of the immature-to-mature cell population

ratio at CR and PR in patients with both R140 (201-023 and 203-002) and R172 (104-036, 201-010 and 201-011) mIDH2. In contrast, no improvement of immature-to-mature ratio was observed in five non-responding patients (**Fig. S3**). In the same patients, we assayed m*IDH2* VAF by NGS in bulk bone marrow mononuclear cells (BMMC) and flow-sorted mature myeloid cells **(Fig. 3B**). In four of five patients achieving CR or PR, m*IDH2* VAF remained stable (201-010, 201-011, 104-036) or increased (201-011) in both populations.

We extended these findings by measuring m*IDH2* VAF in peripheral blood neutrophils prior to enasidenib treatment and at time of CR in seven additional patients who achieved CR (**Fig. 3C,** top panel). In six of seven cases, m*IDH2* VAF remained constant between pre-therapy leukemic cells and neutrophils at CR, consistent with differentiation of m*IDH2* leukemia cells into mature neutrophils. Furthermore, in patient 104-018, the VAF of additional co-associated AML mutations remained unchanged in neutrophils at CR, consistent with enasidenib-mediated differentiation of a transformed leukemic clone (**Fig. 3C,** middle panel). In contrast, in the one patient whose m*IDH2* VAF dropped to 0% in mature neutrophils at CR (104-010), the VAF of other AML-associated mutations showed heterogeneous changes consistent with clonal selection rather than loss of all clonally derived leukemic cells (**Fig. 3C,** top and bottom panels). Next, we investigated the functional status of differentiated leukemic neutrophils with m*IDH2* in three patients who achieved CR **(Table S1)**. In each case, mutant neutrophils demonstrated intact phagocytic activity consistent with restoration of normal granulocyte function **(Fig. 3D).**

*Genomic Predictors of Response to mIDH2 Inhibition*

We assessed whether additional somatic mutations were associated with differential response by performing capture-based NGS of 410 cancer genes on 100 patient samples pre-therapy. Ninety-eight percent of samples contained mutations other than m*IDH2* and 17 co-occurring mutated genes were identified in ≥5% of the 100 patients with mutation data available **(Fig. 4A-B)**. The most frequent co-occurring mutations were in *SRSF2* (45%), *DNMT3A* (42%), *ASXL1*

(27%), *RUNX1* (24%), *NRAS* (17%), and *BCOR* (15%). The prevalence of mutations in this cohort differed from those reported in *de novo* AML, including an increased frequency of adverse risk mutations (*DNMT3A*, *ASXL1*, *RUNX1*) and decreased frequency of favorable prognosis mutations (*NPM1*, *CEBPA)*[26]. Differences were also observed in co-occurring mutations between patients with R140 and R172 m*IDH2* AML **(Fig. 4A and Fig. S4A-B)**. In R140 *mIDH2* patients, co-mutational heterogeneity was higher (60 different mutated genes versus 24 in R172 mIDH2 patients) and significantly more co-occurring mutations were observed (3.6 versus 2.6 mutations per patient in R172 m*IDH2*, p = 0.020, **Fig. S4C**). Some mutated genes were also either exclusively observed (*SRSF2*, n = 45) or enriched in R140 m*IDH2* AML (*RUNX1*, 27.3% versus 14.3% in R172 m*IDH2* AML) or enriched in R172 m*IDH2* AML (*DNMT3A*, 66.7% versus 36.4% in R140 m*IDH2*). This data extends prior work on *de novo* R140 and R172 m*IDH2* AML [13], by showing that R140 and R172 m*IDH2* rrAML are genetically distinct leukemia subtypes.

Analysis of mutational data overlaid with cytogenetics was performed using three different risk classifications of *de novo* AML [13,26,27]. Using the European LeukemiaNet classification, 14% of patients were classified as favorable risk and a disproportionately large number (63%) were classified as intermediate risk (**Fig. 4C**) [27]. Using a recently developed classification scheme by Grimwade et al showed an enrichment of adverse risk patients [26]. Finally, a third classifier developed on a large *de novo* AML cohort [13] revealed an enrichment of patients with mutations in genes regulating splicing/chromatin modifications (48%), and with *TP53* mutations or aneuploidy (21%). Only 14% of patients were categorized as *NPM1* mutation-associated AML, which was reported as the largest AML subset (**Fig. 4D**). Importantly, clinical responses to enasidenib were observed across the risk spectrum in the 72 efficacy-evaluable patients with full genomic/cytogenetic data (**Table S2**).

We next investigated whether the number of co-occurring mutations or specific mutant alleles correlated with enasidenib response. Patients who achieved a response (≥PR or CR) had significantly fewer co-occurring mutations than non-responders ($p < 0.001$, **Fig. 5A**). Segregating patients in three tertiles (≤ 3, 3 to 6, and ≥ 6 co-mutations) revealed a significant difference in ORR for patients with the most versus least co-occurring mutations (ORR 23.3% vs 69.2%, respectively, $p = 0.001$) (**Fig. 5B**). Analysis of co-mutated genes with response indicated a lower, but statistically non-significant, ORR with co-occurring *SRSF2* (34%), *ASXL1* (39%), *RUNX1* (26%), and *NRAS* (19%) mutations (**Table S3**)**.** However, significantly fewer patients with co-occurring *NRAS* mutations achieved CR ($p = 0.0061$; **Table S3**). When the most common mutations known to activate NRAS signaling (G12, G13, or Q61) were analyzed versus ORR, the observed decrease in response rate was statistically significant ($p = 0.002$**, Fig. 5C**). Notably, overall mutational burden was significantly higher ($p < 0.001$) in patients with m*NRAS* (G12, G13, or Q61) and mutations in *NRAS* were frequently subclonal (**Fig. 5D-E**). Analysis of other gene mutations involved in activating MAPK signaling revealed that no patients with m*PTPN11* responded and m*KRAS* was not associated with response (**Table S3**). Together these data suggest that some RAS pathway mutations, either in the dominant, or minor subclone may directly, or indirectly, attenuate responses to mIDH2 inhibition.

**Discussion (727)**

Our study in patients with *mIDH2* rrAML extends previous observations in *de novo* R140 and R172 *mIDH2* AML, confirming that the two *mIDH2* subtypes are genetically distinct with fewer co-occurring mutations in the R172 subtype and *SRSF2* mutations exclusively seen in R140 AML. Not surprisingly, *mIDH2* rrAML patients are enriched for mutations more commonly seen in adverse-risk or secondary AML (e.g., *SRSF2*, *RUNX1,* and *ASXL1)*. Despite this, the ORR with enasidenib was ~40%, with no statistical difference in clinical response rates between R140 and R172 m*IDH2* subtypes [18]. Analysis of patient samples confirms that the preclinical efficacy and mechanism of action of mIDH2 inhibition by enasidenib is through differentiation of AML cells [10,14-16]. Additionally, our data provides the first insight into the genetic basis of primary resistance to enasidenib, which is more likely in patients with higher mutational burden, especially in the RAS/MAPK pathway.

Human AML is composed of a hierarchy of both tumor-propagating leukemic stem cells (LSCs) and more mature non-tumor propagating leukemic cells. Current evidence suggests AML LSCs are arrested at a progenitor or precursor stage of hemopoiesis [28,29]. Preclinical data showed that m*IDH2* and elevated 2-HG blocked hematopoietic differentiation [6,8-10]. Our observations demonstrate enasidenib promotes terminal differentiation of m*IDH2* leukemic cells of granulocytic lineage in patients who achieve complete or partial response. Furthermore, we observed *ex-vivo* phagocytic function in differentiated m*IDH2*-containing neutrophils. Taken together, these observations are clinically important and likely explain the lower frequency of infections in patients in CR, who in most cases have *mIDH2* circulating neutrophils.

Our studies also demonstrate decreases in m*IDH2* below a detectable limit in a subgroup of patients. Both observations support differentiation as the mechanism of action of enasidenib monotherapy. In the former case, where m*IDH2* cells persist, one hypothesis is that m*IDH2* LSCs are not eradicated but differentiate to give rise to m*IDH2*-containing neutrophils. In the

latter case, where molecular CR was achieved in the R140 group of patients, m*IDH2* inhibition may result in terminal or near terminal exhaustion through differentiation of the m*IDH2* clone. The differential effects may be due to the specific cellular and genetic contexts of the *IDH2* mutation and additional work will be required to dissect the mechanisms accounting for these observations. Although enasidenib responses are clinically durable, the genetic heterogeneity observed in our patients suggests combination with other therapies may be required to achieve long-term disease remission in more patients. This is reminiscent of the impressive, but not durable, activity of ATRA monotherapy in acute promyelocytic leukemia [30]. Finally, it is intriguing and unclear why CR is achieved when the *mIDH2* clone(s) are subclonal; this requires further mechanistic studies of cell autonomous and cell non-autonomous effects of *IDH2* mutations in AML.

Pre-therapy serum 2-HG levels have been suggested as a biomarker for chemotherapy response in m*IDH2* patients [1-4]. Our data demonstrates this is not the case in targeted therapy and is due to the ability of enasidenib to inhibit the mIDH2 enzyme regardless of whether a patient attains a clinical response. Consistent with this hypothesis the level of suppression of 2-HG is not prognostic of response. Furthermore, though the extent of 2-HG suppression is more variable, and maximal suppression takes longer to achieve in R172 *mIDH2* patients, clinical responses are observed in both m*IDH2* subtypes. Our data demonstrate that although 2-HG suppression is likely a requirement for response, the extent of 2-HG suppression does not predict clinical response, and primary resistance to enasidenib is not due to an inability to suppress mIDH2 enzyme activity.

These data suggest other factors determine clinical response to enasidenib. Patients with a higher mutational burden and/or co-occurring mutations in the RAS pathway were observed to be less likely to respond to mIDH2 inhibition. It is unclear if constitutive activation of the RAS pathway imposes a 2-HG-independent differentiation block or whether mutations in *RAS* and

other signaling pathways are a marker of overall higher mutational burden and other mechanisms of 2-HG-independent differentiation arrest. Notably, *NRAS* mutations were frequently present in a minor subclone and this intriguing observation requires further investigation. While this is only a subgroup analysis of a large single-arm experience, taken together, the clinical response and translational data demonstrate that single-agent mIDH2 inhibition by enasidenib in rrAML represents a critical and novel differentiation therapy. It also provides the platform for future combination therapy regimens to optimize clinical response and further improve outcomes in m*IDH2* AML.

## References and Notes


1. Gross S, Cairns RA, Minden MD, et al. Cancer-associated metabolite 2-hydroxyglutarate accumulates in acute myelogenous leukemia with isocitrate dehydrogenase 1 and 2 mutations. *J Exp Med*. 2010;207(2):339-344.
2. Ward PS, Patel J, Wise DR, et al. The common feature of leukemia-associated IDH1 and IDH2 mutations is a neomorphic enzyme activity converting alpha-ketoglutarate to 2-hydroxyglutarate. *Cancer Cell*. 2010;17(3):225-234.
3. Fathi AT, Sadrzadeh H, Borger DR, et al. Prospective serial evaluation of 2-hydroxyglutarate, during treatment of newly diagnosed acute myeloid leukemia, to assess disease activity and therapeutic response. *Blood*. 2012;120(23):4649-4652.
4. Janin M, Mylonas E, Saada V, et al. Serum 2-hydroxyglutarate production in IDH1- and IDH2-mutated de novo acute myeloid leukemia: a study by the Acute Leukemia French Association group. *J Clin Oncol*. 2014;32(4):297-305.
5. Xu W, Yang H, Liu Y, et al. Oncometabolite 2-hydroxyglutarate is a competitive inhibitor of alpha-ketoglutarate-dependent dioxygenases. *Cancer Cell*. 2011;19(1):17-30.
6. Lu C, Ward PS, Kapoor GS, et al. IDH mutation impairs histone demethylation and results in a block to cell differentiation. *Nature*. 2012;483(7390):474-478.
7. Figueroa ME, Abdel-Wahab O, Lu C, et al. Leukemic IDH1 and IDH2 mutations result in a hypermethylation phenotype, disrupt TET2 function, and impair hematopoietic differentiation. *Cancer Cell*. 2010;18(6):553-567.
8. Losman JA, Looper RE, Koivunen P, et al. (R)-2-hydroxyglutarate is sufficient to promote leukemogenesis and its effects are reversible. *Science*. 2013;339(6127):1621-1625.
9. Wang F, Travins J, DeLaBarre B, et al. Targeted inhibition of mutant IDH2 in leukemia cells induces cellular differentiation. *Science*. 2013;340(6132):622-626.
10. Kats LM, Reschke M, Taulli R, et al. Proto-oncogenic role of mutant IDH2 in leukemia initiation and maintenance. *Cell Stem Cell*. 2014;14(3):329-341.
11. Green CL, Evans CM, Zhao L, et al. The prognostic significance of IDH2 mutations in AML depends on the location of the mutation. *Blood*. 2011;118(2):409-412.
12. Molenaar RJ, Thota S, Nagata Y, et al. Clinical and biological implications of ancestral and non-ancestral IDH1 and IDH2 mutations in myeloid neoplasms. *Leukemia.* 2015;29(11):2134-2142.
13. Papaemmanuil E, Gerstung M, Bullinger L, et al. Genomic Classification and Prognosis in Acute Myeloid Leukemia. *N Engl J Med*. 2016;374(23):2209-2221.
14. Yen K, Wang F, Travins J, et al. AG-221 Offers a Survival Advantage In a Primary Human IDH2 Mutant AML Xenograft Model. *Blood* 2013;122:240.
15. Shih AH, Shank KR, Meydan C, et al. AG-221, a Small Molecule Mutant IDH2 Inhibitor, Remodels the Epigenetic State of IDH2-Mutant Cells and Induces Alterations in Self-Renewal/Differentiation in IDH2-Mutant AML Model in Vivo. *Blood* 2014 124:437.
16. Quivoron C, David M, Straley K, et al. AG-221, an Oral, Selective, First-in-Class, Potent IDH2-R140Q Mutant Inhibitor, Induces Differentiation in a Xenotransplant Model. *Blood* 2014;124:3735.
17. Shih AH, Meydan C, Shank K, et al. Combination Targeted Therapy to Disrupt Aberrant Oncogenic Signaling and Reverse Epigenetic Dysfunction in IDH2- and TET2-Mutant Acute Myeloid Leukemia. *Cancer Discov*. 2017.
18. Stein E, DiNardo C, Pollyea D, et al. Enasidenib in mutant-IDH2 relapsed or refractory acute myeloid leukemia. *Submitted*. 2016.
19. Walter RB, Gooley TA, Wood BL, et al. Impact of pretransplantation minimal residual disease, as detected by multiparametric flow cytometry, on outcome of myeloablative hematopoietic cell transplantation for acute myeloid leukemia. *J Clin Oncol*. 2011;29(9):1190-1197.
20. Walter RB, Gyurkocza B, Storer BE, et al. Comparison of minimal residual disease as outcome predictor for AML patients in first complete remission undergoing myeloablative or nonmyeloablative allogeneic hematopoietic cell transplantation. *Leukemia*. 2015;29(1):137-144.
21. He J, Abdel-Wahab O, Nahas MK, et al. Integrated genomic DNA/RNA profiling of hematologic malignancies in the clinical setting. *Blood*. 2016;127(24):3004-3014.
22. Fan B, Chen Y, Wang F, et al. Evaluation of Pharmacokinetic-Pharmacodynamic (PKPD) Relationship of an Oral, Selective, First-in-Class, Potent IDH2 Inhibitor, AG-221, from a Phase 1 Trial in Patients with Advanced IDH2 Mutant Positive Hematologic Malignancies. *Blood*. 2014;124(21):3737.

23. Fan B, Chen Y, Wang F, et al. PHARMACOKINETIC/PHARMACODYNAMIC (PK/PD) EVALUATION OF AG-221, A POTENT MUTANT IDH2 INHIBITOR, FROM A PHASE 1 TRIAL OF PATIENTS WITH IDH2-MUTATION POSITIVE HEMATOLOGIC MALIGNANCIES. *Haematologica*. 2015;100 (1 Supplement):379.
24. Gao Y, Fan B, Le K, et al. Evaluation of the Pharmacokinetics of AG-221, a Potent Mutant IDH2 Inhibitor, in Patients with IDH2-Mutation Positive Advanced Hematologic Malignancies in a Phase 1/2 Trial. *Blood*. 2015;126(23):2509.
25. DiNardo C, de Botton S, Stein E, et al. Determination of IDH1 Mutational Burden and Clearance Via Next-Generation Sequencing in Patients with IDH1 Mutation-Positive Hematologic Malignancies Receiving AG-120, a First-in-Class Inhibitor of Mutant IDH1 *Blood*. 2016;128(22):1070.
26. Grimwade D, Ivey A, Huntly BJ. Molecular landscape of acute myeloid leukemia in younger adults and its clinical relevance. *Blood*. 2016;127(1):29-41.
27. Mrozek K, Marcucci G, Nicolet D, et al. Prognostic significance of the European LeukemiaNet standardized system for reporting cytogenetic and molecular alterations in adults with acute myeloid leukemia. *J Clin Oncol*. 2012;30(36):4515-4523.
28. Goardon N, Marchi E, Atzberger A, et al. Coexistence of LMPP-like and GMP-like leukemia stem cells in acute myeloid leukemia. *Cancer Cell*. 2011;19(1):138-152.
29. Quek L, Otto GW, Garnett C, et al. Genetically distinct leukemic stem cells in human CD34- acute myeloid leukemia are arrested at a hemopoietic precursor-like stage. *J Exp Med*. 2016;213(8):1513-1535.
30. Warrell RP, Jr., Frankel SR, Miller WH, Jr., et al. Differentiation therapy of acute promyelocytic leukemia with tretinoin (all-trans-retinoic acid). *N Engl J Med*. 1991;324(20):1385-1393.

**Acknowledgments:** MA, LQ, AS, MR, BM and NFR performed experiments. ES, SB and MD coordinated sample collection. All authors contributed to experimental design, analyzed data and edited the manuscript. PV, RL and MA wrote the manuscript. AT led all translational studies and analysis efforts. We thank Sung Choe (Agios Pharmaceuticals) for helpful discussions, operational assistance and data cleaning. LQ was supported by a fellowship from Celgene. PV and LQ acknowledge funding from the MRC (MHU Award G1000729, MRC Disease Team Award 4050189188), CRUK (Program Grant to PV C7893/A12796, CRUK program grant to BG C1163/A21762), Bloodwise (Specialist Program 13001) and the Oxford Partnership Comprehensive Biomedical Research Centre (NIHR BRC Funding scheme). This work was supported by grant R01CA172636-01 to RLL, by grant U54OD020355-01 to RLL, by a supplement to P30CA008748 to RLL, and MSK cores used to perform studies included in this work are supported by P30CA008748. RLL is a scholar of the Leukemia and Lymphoma Society. AHS is supported by the Conquer Cancer Foundation and by

NCIK08CA181507. Authors acknowledge helpful advice and review of drafts by Celgene and Agios colleagues, especially Krishnan Viswanadhan, Samantha Good, and Kyle Macbeth.

**Figures:**

**Fig. 1. mIDH2 Inhibition Is Associated with Potent Reduction of 2-HG in mIDH2 AML**

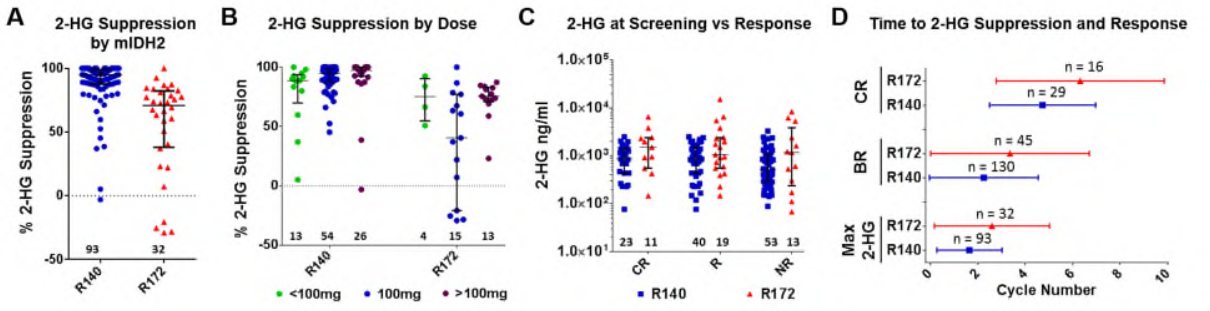


**(A)** Dot plot with median and interquartile range showing maximum 2-HG suppression (% change from baseline) in blood observed in patients segregated by R140 and R172 mIDH2. Numbers indicate number of patients from each genotype graphed.

**(B)** Dot plot with median and interquartile range showing maximum 2-HG suppression (% change from baseline) observed in patients segregated by total daily dose received (<100 mg in green, 100mg in blue, >100 mg in purple) and stratified by R140 and R172 mIDH2.

**(C)** Dot plot with median and interquartile range showing blood plasma 2-HG (ng/ml) at screening in patients segregated by best response achieved and stratified by R172 (red) and R140 (blue) mIDH2. Response (R) is defined as either complete remission (CR), CR with incomplete count recovery (CRi), CR with incomplete platelet count recovery (CRp), morphologic leukemia-free state (MLFS) or partial remission (PR). NR (no response) is defined as stable disease (SD) or progressive disease (PD).

**(D)** Whisker plot indicating mean and standard deviation of cycle to CR, Best Response (BR) or maximum 2-HG suppression (Max 2-HG) stratified by R172 (red) and R140 (blue) mIDH2.